Zinc Oxide Modified Carbon Nanotubes Prepared Utilizing Solution Gelation Process: Characterization and Sensing Application

Jumana Kareem Buraihi Mahdi[1], Hikmat Adnan Banimuslem[2]*
[1], [2]University of Babylon, Babylon, Iraq
Email: hikmatadnan@gmail.com

Abstract
A hybrid material of zinc oxide and carbon nanotubes have been synthesized via a sol-gel process using zinc acetate dehydrate and acid modified multiple-wall carbon nanotubes. Very fine nanoparticles were achieved as color of solution and SEM images indicated. Thin films were deposited utilizing spray pyrolysis technique onto glass substrate as well as indium tin oxide coated glass to perform sandwich device structure. Samples were heated at different annealing temperatures and only samples heated with 500 oC have shown reasonable results. The optical energy gap has been investigated using UV-Visible absorption spectroscopy and Tauc calculations. Temperature dependence conductivity has been investigated in the range of 20 to 200 oC. NO2 gas interaction with the samples was studied using homemade chamber.
Keywords: ZnO, CNT, Sol Gel, Spray pyrolysis, Activation energy, Sensor.

1. Introduction

Zinc oxide (ZnO) is considered as one of the most promising semiconducting materials recently with a very good optical photo-transparency in the range of visible light, energy band gap ~ 3.3 eV and 60 meV exciton binding energy [1,2]. Thin films of ZnO have been explored in the very recent years as transparent conducting oxides (TCO) as of their promising electrical and optical characteristics in combination with a high thermal conductivity, high electron mobility, decent transparency, wide and direct energy band gap at room environment and large exciting binding energy [3]. In addition, growing ZnO in the nanostructure utilizing many different procedures is quite simple which makes ZnO appropriate for a very wide range of applications such as light-emitting diodes [4], varristors [5], solar panels [6] and odorant sensors [7]. Additionally, zinc oxide is a talented material for short wavelength optoelectronics, especially for UV light emitting device and laser diodes (LDs), due to the large exciton binding energy [8]. Zinc oxide thin films are full-grown by many different methods includes pulsed laser deposition (PLD) [9,10], magnetron sputtering [11], MOCVD [12,13], spray pyrolysis [14] and sol–gel process [15,16]. Carbon nanotubes (CNTs), on the other hand, have drawn great attention since they were discovered because of their fascinating structural, mechanical, electronic, optical and thermal properties, and excellent chemical stability [17], leading to potential high-technology applications such as biosensor,[18] super capacitor, [19] hydrogen storage [20] and field emission devices[21].
Although there are plenty of methods that employed to prepare zinc oxide, sol–gel technique is one of the most popular solutions processing method for producing metal oxide nanoparticles due to the effectiveness of having very fine nanoparticles on a side and the easiness of processing wet technique thereafter on the other side to produce homogeneous and uniform thin films [22,23]. Amongst all wet techniques used to perform thin films, spray pyrolysis is very convenient method especially with the solutions that are not volatile. Spray is a simple and low-cost technique for the preparation of thin films; it has capability to produce large area, high quality adherent films of uniform thickness. spray technique does not require high quality targets and /or substrates nor does require vacuum at any stage, which is a great advantage if the technique is to be scaled up for industrial applications; the deposition rate and the thickness of the films can be easily controlled over a wide range by changing the spray parameters [24]. In this study, zinc oxide has been synthesized using sol-gel method and modified using carbon nanotubes. Optical and structural properties were investigated. Sensing performance for the fabricated devices has been examined due different odorants as in situe detection sensors.

2. Materials and Methods

In this work, ZnO thin films were prepared by sol–gel method. Zinc acetatedehydrate, 2-methoxyethanol and monoethanolamine (MEA) have been used as starting, precursor and catalyst materials. 21.9 g of zinc acetate dehydrate was first dissolved in a mixture of (133ml) of 2-methoxyethanol and (6.03ml) of MEA solution at room temperature. The molar ratio of MEA to zincacetate was maintained at 1.0 and the concentration of zinc acetate was 0.75 M. The solution was stirred at 60 oC for 2 h to yield a clear and homogeneous solution, which served as the precursor solution. The color was turned to dark yellow indicating very fine colloidal nanoparticles was attained [25]. Same process was repeated with

doi.org/10.31838/hiv23.02.43 Received: 10.10.22, Revised: 02.11.22, Accepted: 03.12.22

the addition of 14 mg multi walled carbon nanotubes with the Zinc acetatedehydrate, 2-methoxyethanol and (MEA) . Films were deposited onto glass and ITO glass using spray coating. The glass substrates are for optical and structural characterizations, whereas the ITO substrates were further made as sandwich structure devices by thermal evaporating aluminum top electrodes for performing electrical investigations and sensor measurements. After being deposited by spray coating, the films were annealed at 250 and 500 oC at a programmable furnace.

3. Characterization

UV-Visible Absorption Spectroscopy is used to study the optical properties and energy gaps calculations. Fourier Transform Infrared technique has been employed to investigate the chemical functional groups of the prepared samples. X-Ray Diffraction has been utilized to reveal the structure and grain size calculations. Morphology of the prepared samples was explored using scanning electron microscopy technique. Keithly semiconductor characterization system has been utilized to investigate the electrical properties. Homemade instrument was used to carry out the sensor measurements.

4. 4. Results and Discussion

UV-Visible Absorption Spectra

The size of nanoparticles plays significant role in varying all characteristics of materials. Therefore, size developments of semiconductors' particles became essential to investigate the material properties [26]. One of the most important equipment to examine the optical properties of nano-sized materials is the UV-Visible absorption spectroscopy. Figure (1) shows the absorbance spectra of the ZnO and ZnO/CNT hybrid thin films annealed at 250 and 500 oC in the wavelength range of (300-1000) nm. It was found that the absorption appeared in the UV range 300 nm. This phenomenon is arising from the intrinsic electron transition between higher occupied molecular orbital (HOMO) and lower unoccupied molecular orbital (LUMO). Another exitonic bands were found at about 380 nm due to the nano size particles. This peak was very clear in the samples annealed at 500 oC (figure (1) b and c) suggesting the successful formation of ZnO nanoparticles at this range of annealing temperature [27].

The loading of CNT to the samples results in red shift in the absorption spectra indicating the successful anchoring of nano-size ZnO onto the side wall of carbon nanotubes. In addition, the effective utilization of the created electron-hole pairs via carbon nanotube modification took place. Another finding that should be given attention is the shape of the spectra. By looking to the spectra of ZnO/CNT which heated at 250 oC, it can clearly be seen that the curve is likely to be similar to the spectra of pristine CNT which is feature less as reported previously [28]. However, at 500 oC, the spectra of ZnO/CNT showed the same characteristics of ZnO spectra suggesting successful decorating of nanoparticles onto the CNTs.

The optical band gap (Eg) was derived assuming a direct transition between the edge of the valence and conduction band as there have been linear regions in all curves. The plot of (αhν)2 as a function of the energy of incident radiation (hν) has been shown in Figure (2). The energy band gap is obtained from intercept of the extrapolated linear part of the curve with the energy axis and found to be; 3.13 and 2.86 for ZnO and ZnO/CNT samples annealed at 250 oC and 3.18 and 2.53 for ZnO and ZnO/CNT samples annealed at 500 oC respectively. There is a variation of the band gap energy of ZnO and ZnO/CNT where the optical band gap (Eg) of the samples which contains CNT decreases giving intense evidence of CNT presence which narrow the band gaps of ZnO, allowing better absorption [29]. The direct band gap of the ZnO films was decreases as the annealing temperatures increases, this is expected to take place due to the variation in lattice defects and stress. The compressed lattice is expected to provide a wide band gap because of the increased repulsion between the oxygen 2p and the zinc 4s bands [30].

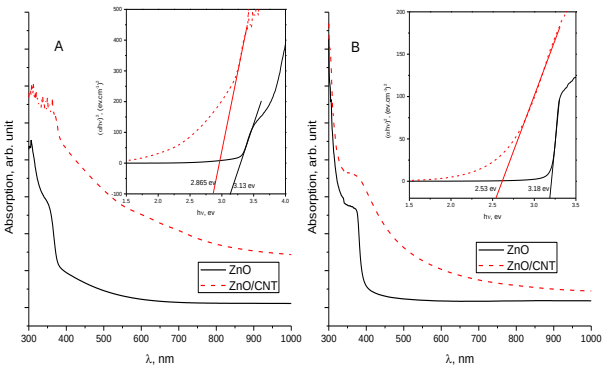

Figure 1. UV-Visible absorption spectra of ZnO (solid lines) and ZnO/CNT hybrid (dashed lines) thin films annealed at (A) 250 °C and (B) 500 °C. The inset represents the Tauc's plot of photon energy.

Thermal Dependence Conductivity

Thermal dependence conductivity has been investigated for all samples with ITO bottom electrodes and Al as top electrodes using Keithly (2400) semiconductor characterization system for the temperature range between room temperature to 200 oC. By looking to the samples of ZnO and ZnO/CNT which heated at 250 oC, it can clearly be seen that it didn't give any clear results and no obvious semiconducting performance was exhibited, The reason for this is that zinc oxide was not achieved, meaning that it did not work as a semiconductor even in the presence of carbon nanotubes. However, samples annealed at 500 oC

have shown typical behavior of zinc oxide semiconductor.

The temperature dependence conductivity has been studied using Arrhenius equation [31,32,33,34].

$\sigma=\sigma_{\circ}exp[Ea/K_BT]$ (1)

where (σo) ; the pre-exponential factor, (Ea); the activation energy for electrical conductivity corresponding to the energy difference between donor level and conduction level, (KB); Boltzmann constant (1.38 × 10-23) J/K and (T); temperature in Kelvin.

The schemes of conductivity against temperature of ZnO nano-structured film heated at 500oC is exhibited in figure 2(a and b). It has been obviously seen that 3 different areas are shown in this figure which are I, II and III. These regions are corresponded to not the same conduction mechanisms. In the regions I, II and III, the electrical conductivities increase with the increasing of temperature. This is suggested to happen as more chargge carriers overcome the barrier of activation energy as a result of rising the temperature and therefore, this carrier enhances the electrical conductivity.

(EI), (EII), (EIII) values for regions I, II and III have been calculated from the linear parts of figure 2. The obtained values were 0.448, 0.081 and 0.418 eV for ZnO and 0.136, 0.199 and 0.491 for ZnO/CNT materials respectively. The value of the activation energy for region I obtained from conductivity data is small in contrast with optical band gap energy. This could be interpreted as the optical energy band gap corresponded to another transaction while the activation energy corresponds to the energy necessary for conduction from one site to another. In addition, the foundation of different temperature dependence regions indicate the existence of two donor levels. These levels are named as the shallow level and deep donor levels in the energy band gap of the ZnO. The value of EI corresponds to the shallow donor level, while the value of EIII corresponds to the deep donor level [35]. Therefore, it is estimated that in region III, the electrical conductivity of ZnO film is thermally motivated from the deep donor level to the lower conduction band. The domination of hopping mechanism on the second region of the arc is quite obvious where the electrons have no abundant energy to jump directly. However, electrons in this part of the conduction plot is hopping from the higher ground level to temporary level and then to the lower conduction level [35]. Therefore, the conductivity shows a decrease as charge carriers are depleted ionized from the shallow donor level with the rise of temperature up to activation of charge carrier in deep donor level start. Furthermore, Lee et al. [36] reported that the conductivity for nanophase ZnO having particle size of 60 nm is in the range 2×10-6 to 2×10-4 S/cm at 450–600 oC. The increase in conductivity of ZnO nanostructured thin film studied can be explained as the conductivity of the ZnO film is attributed to the trapping of electrons in the grain boundaries. By comparing models of pure ZnO with models that contain carbon nanotubes ZnO/CNT, which have been represented in figure 2, it can clearly be seen that the transition region is almost very small, and the deviation is not sharp. CNT can create more trapping levels which at the same time these levels work as donor levels leading to electron transfer more easily and that interpret the smallest activation energy shown in the samples having CNT.

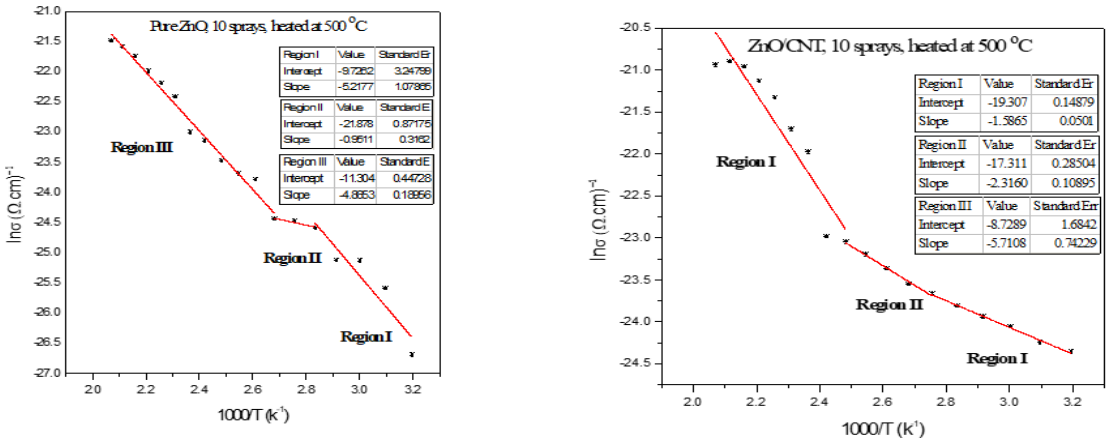

Figure 2. Arrhenius Plot of ln σ vs. 1000/T of pure ZnO and hybrid nanostructured thin film at 500 °C annealing temperature.

Fourier Transform Infrared (FTIR)

Figure 3 shows the FTIR spectra of the ZnO and ZnO/CNT hybrid materials. The inset to the figure 3 represents the sigma aldrich FTIR of ZnO. As obviously can be seen that, there is a high similarity between the prepared ZnO spectrum and the sigma's one indicated excellent purity for the ZnO nanoparticles synthesized in this study. The spectra obtained have clearly shown the Zn-O absorption peak near 546 cm-1. The absorption bands at 3450 and 2923 cm-1 are attributed to O-H vibration stretching from Zn-O-H sorts and C-H stretching vibration correspondingly [37,38,39,40]. The free O-H stretching bond at 3450 cm-1 arises due to reaction of ZnO nanoparticles and hydroxide group. It is worth mentioning that the color of solution in a mixture of 2-methoxyethanol and monoethenolamine is orange where as that of solution of alcohol is transparent. The peak at 715

cm-1 which appeared only in the spectrum of the hybrid material, is may be attributed to the carbon-carbon stretching of carbon nanotubes [40]. This

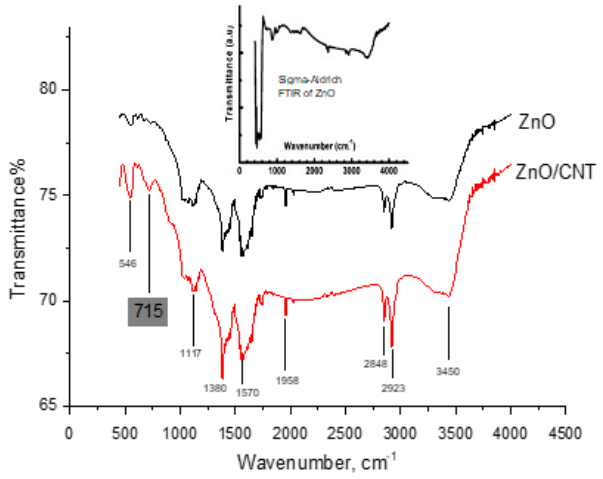

Figure 3. The FTIR spectra of ZnO and ZnO/CNT prepared by sol-gel method. The inset is sigma Aldrich spectrum of ZnO.

5. Morphology

Scanning electron microscopy technique has been used to study the topography of the samples prepared in this work. At low magnification images, samples annealed at 250o C, surface has examined a cracked surface while those annealed at 500o C show quite homogeneous surface indicating higher temperature is needed for the ZnO thin films to be achieved adequately. These images are presented in figure 4 for the clarity.

In addition irregular thin films have been produced when heated at 250o C while spherical-type morphology was shown by samples treated at 500o C for half an hour. Figure 5 represents the uniform arrangement of ZnO grains with nano scale down to ~ 22nm. Zinc oxide usually tends to form nano-sphere structure [41], rod-like structure [42], or nano-

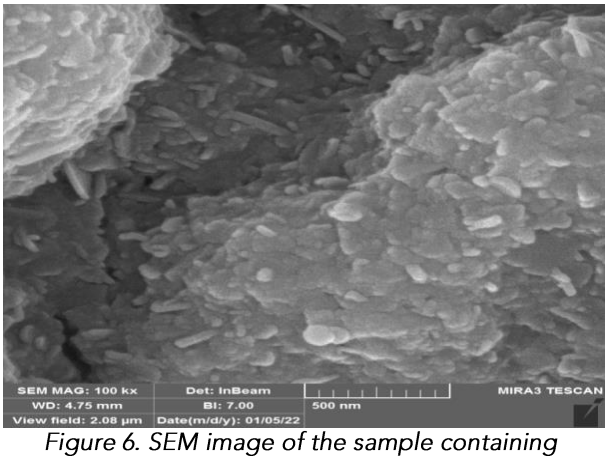

Figure 6. SEM image of the sample containing MWCNTs.

6. Gas sensing

Samples have been exposed to NO2 at the concentration of 100 ppm using homemade resistive sensing system at room temperature. Gas sensors with very high responding to odorants, at the same

peak indicated the successful decorating of ZnO nanoparticles onto sidewall of carbon nanotubes

flower structure [43] depending on preparation method, coating and heat treatment.

Figure 6 shows the SEM images of the samples containing CNT have shown clear tubes decorated by ZnO nanoparticles confirming the successful anchoring of the ZnO onto side-wall of the carbon nanotubes. This foundation was also reported elsewhere [44]

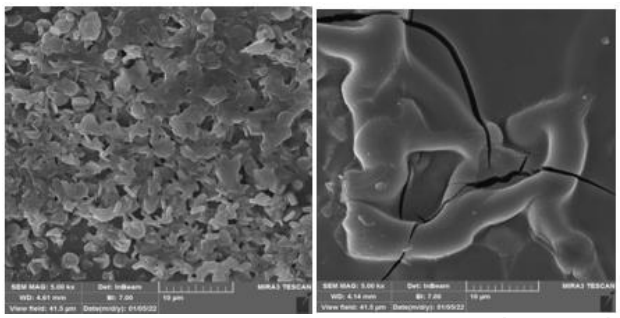

Figure 4. SEM images at 5kx (10 µm) magnification of sprayed ZnO thin films prepared by sol-gel (a) annealed at 250o C and (b) annealed at 500o C.

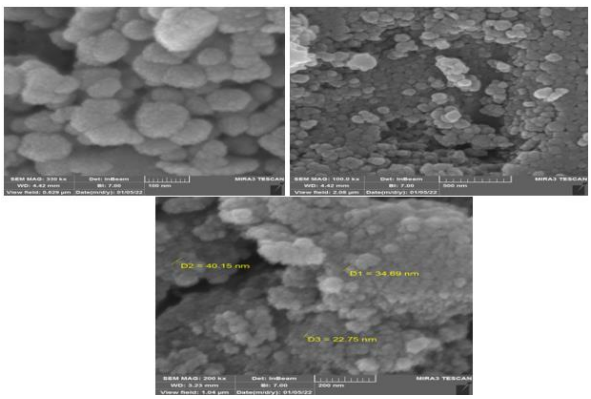

Figure 5. The spherical like structure of ZnO at different magnifications (a) 330 kx (100nm), (b) 100 kx (500 nm), (c) shows the grain size of the nanoparticles.

time working at room temperature are considered as more attractive devices because of their low power consumption and long-lasting stability [45]. Until meantime, zinc oxide as semiconducting oxide is well known as potential resistance-based gas sensor. However, Higher operating temperature becomes the drawback of its widespread applications in the area of real time gas detection, particularly, in combustible and volatile gas environment. In this contest, global research efforts were keen to reduce the temperature that the sensor device working on and the literature [46] has comprehensively reviewed the room temperature gas sensing properties of ZnO. Much more attention is predominantly waged to the effective approaches that produce room temperature gas detection of ZnO based gas sensors, mostly including doping with other materials, morphology enhancements and light initiations. Finally, some perceptions for future enquiry on room temperature gas detection resources are deliberated as well [47].

Figure 7 shows the response vs. time of ZnO and

hybrid films towards NO2. It is obviously seen that ZnO are not reversible as the resistance has not come to the initial value after the gas being disposed from the sample surface. Whereas, the hybrid film have shown quite interesting performance due gas interaction which make them promising candidate for sensing applications. It is expected that the presence of CNT in the composite film inhibits the diffusion of gas molecules inside the film and most interaction takes place on the surface of the film [48]. The response and recovery times have been calculated as 90% of the maximum response after gas on and 90% of the returning to initial state after gas off and found to be 10 and 150 second respectively.

7. Conclusion

Zinc oxide and hybrid of zinc oxide and carbon nanotubes thin films have been prepared by the mean of sol gel and spry pyrolysis techniques. The UV-visible absorption spectra revieled that carbon nanotubes causes a red shift and results in reducing the optical band gap by ~ 1 ev. The temperature dependence conductivity has shown three conduction mechanisms and no recombination allowed in the films with carbon nanotubes. The grain size of the prepared zinc oxide was in the range of ~ 20-40 nm as the SEM images conducted. The FTIR spectra has exhibited a very obvious similarity between the prepared ZnO and the sigma Aldrich one. NO2 gas interaction with the synthesized devices has been studied and the results show that the existence of carbon nanotubes reduces the chemical interaction and so complete recovery achieved after purging the samples with fresh air. The response time and recovery time were calculated and found to be 10 and 150 seconds respectively.

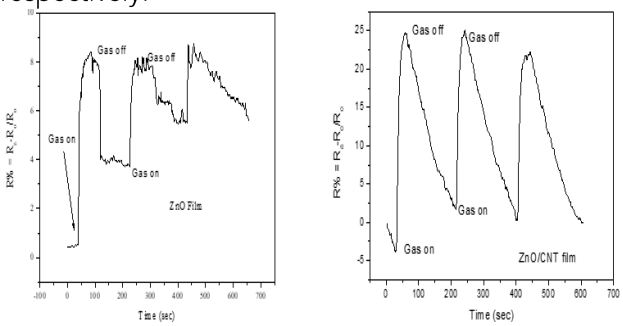

Figure 7. The time dependency of the response upon exposure to 100 ppm NO2 gas for the ZnO and hybrid films.

References

[1] L. Xu, X. Li, Y. Chen, and F. Xu, Journal of Applied Surface Science. 257, 4031–4037 (2011).
[2] W. S. Han, Y.Y. Kim, B. H. Kong, and H. K. Cho, Journal of Thin Solid Films. 517, 5106 -5109 (2009).
[3] Z. L. Wang, Journal of Materials Today. 7, 26-33 (2004).
[4] J. Gao, A.J. Heeger, J.Y. Lee, and C.Y. Kim, Journal: Synthetic Metals. 82, 221-223 (1996).
[5] N.T. Hung, N.D. Quang, and S. Bernik, Journal of Materials Research. 16, 2817 - 2823 (2001).
[6] N.F. Cooray, K. Kushiya, A. Fujimaki, D. Okumura, M. Sato, M. Ooshita, and O. Yamase, Japanese Journal of Applied Physics. 38, 6213 (1999).
[7] R. Paneva and D. Gotchev, Journal: Sensors and Actuators A: Physical. 72, 79-87(1999).
[8] C. M. Lieber, Journal: Solid State Communications. 107, 607-616 (1998).
[9] J.A. Sans, A. Segura, M. Mollar and B. Mari, Journal of Thin Solid Films. 453, 251-255 (2004).
M. Durmuş, S. Tuncel, A.A. Esenpınar, A.G. Gürek and V. Ahsen, Key. Eng. Mat. 605, 461-464, (2014).
[29] M.M. Mohamed and M.A.Ghanim, M.Khairy, E.Naguib and N.H.Alotaibi , Applied surface science. 487, 539-549 (2019).
[10] G.H. Lee, T.H.Kim, C.Yoon and S.Kang, Solid State Commun. 128, 1922-1926 (2008).
[11] J.B. Lee, S.H.Kwak and H.J. Kim, Journal of Thin Solid Films. 423, 262-266 (2003).
[12] J.Ye, S.Gu, S.Zhu, T.Chen, L.Hu, F.Qin, R.Zhang, Y.Shi and Y.Zheng, Journal of Crystal Growth. 243, 151-156 (2002).
[13] K.S. Kim, et al., Journal of Mater. Sci. and Eng. B. 98, 30 (2003).
[14] P. Puspharajah, S. Radhakrishna and A. K. Arof , Journal of Mater. Sci. 32, 3001-3006 (1997).
[15] G.K. Paul, S. Bandyopadhyay, S.K. Sen and S. Sen, Journal of Mater. Chem. Phys. 79, 71-75 (2003).
[16] G.G. Valle, P. Hammer, S.H. Pulcinelli and C.V. Santilli, Journal of Cer. Soc. Eur. 24, 81 (2004) .
[17] A. krueger, Carbon Materials and Nanotechnology, (WILEY-VCH Verlag GmbH &Co.KGaA, germany, 2010), pp.123-126.
[18] D. Odaci, A. Telefoncu, and S. Timur, Sens. Actuators, B. 132, 159-165 (2008).
[19] S. Wei, W. P. Kang, J. L. Davidson, and J. H. Huang, Diam. Relat. Mater. 17, 906-911 (2008).
[20] Y. Chen, D. T. Shaw, X. D. Bai, E. G. Wang, C. Lund, W. M. Lu and D. D. L. Chung, Appl. Phys. Lett. 78, 2128 (2001).
[21] J. Y. Pan, C. Y Chen, Y. L. Gao, and C. C. Zhu, Displays. 30, 114-118 (2009).
[22] T.H. Mahato, G.K. Prasad, B.S.J. Acharya, A.R. Srivastava and R. Vijayaraghavan, Journal of Hazardous Materials. 165, 928-932. (2009).
[23] H. Benhebal, M. Chaib, T. Salomon, J. Geens, A. Leonard, S.D Lambert., M. Crine and B. Heinrichs, Alexandria Engineering Journal. 52, 517-523, (2013).
[24] C.M. Lampkin, Prog. Cryst. Growth Characterization of Materials. 1,585-589 (1979).
[25] L. Znaidi, Materials Science and Engineering: B. 174, 18–30, (2010).
[26] A, K.Zak, R. Razali, W.H. Abd Majid and M.Darroudi, International journal of nanomedicine. 6, 1399-1403 (2011).
[27] S.Talam, S.R.Karumuri and N.Gunnam, International Scholarly Research Network. 1, 1-6 (2012).
[28] H. Banimuslem, A. Hassan, T. Basova, I. Yushina,
[30] D. D. Mulmi, A. Dhakal and B. R. Shah, Nepal

Journal of Science and Technology. 15, 111-116 (2014).
[31] D. K. Schroder, Semiconductor Material and Device Characterization, (John Wiley & Sons, New York, 1998), pp.38-40.
[32] D. Newman, Semiconductor physics and devices, Basis Principles, (Richard, University of New Mexico, 1992), pp. 211.
[33] A. H. Jassim and H.A. Banimuslem, Nano Hybrid and Comp. trans. Tech. publications LTD. 29, 22 (2020)
[34] G. Busch, and H. Schade, Lectures on Solid State Physics, (pergamon press, New York, 2013), pp.357-368.
[35] N.T. Hung, N.D. Quang and S. Bernik, Journal of Materials Research. 16, 2817- 2823 (2001).
[36] J. Lee, J.H. Hwang, J.J. Mashek, T.O. Mason, A.E. Miller and R.W. Siegel, Journal of Materials Research. 10, 2295-2300, (1995).
[37] R.K. Thareja and S. Shukla, Applied Surface Science. 235, 8889 (2007).
[38] A. Becheri, M. Durr, P.L. Nostro and P. Baglioni, Journal of Nanoparticle Research. 10, 679 (2008).
[39] R.M. Alwan, Q.A. Kadhim, K.M. Sahan, R.A. Ali, R.J. Mahdi, N.A. Kassim and A.N. Jassim, Nanoscience and Nanotechnology. 5, 1 (2015).
[40] M.M. Mohamed, M.A.Ghanem, M. Khairy, E. Naguib, and N.H. Alotaibi, Applied Surface Science. 487, 539 (2019).
[41] M. Fakhar-e-Alam, S. Rahim, M. Atif, M.H. Aziz, M.I. Malick, S.S.Z. Zaidi, R. Suleman and A. Majid, Laser Physics Letters. 11, 025601 (2013).
[42] A.M. Nahhas, American Journal of Nanomaterials. 6, 15 (2018).
[43] H. Chen, X. Wu and G. Shen, Nanoscale Research Letters. 5, 570 (2010).
[44] V.K. Gupta, S. Rostami, H. Karimi-Male, F. Karimi, M. Keyvanfard, and T.A. Saleh, Int. J. Electrochem. Sci. 10, 1517 (2015).
[45] L. Zhu and W. Zeng, Sensors and Actuators A: Physical. 1, 267 (2017).
[46] L. Zhu, L. Yanqiong and Z. Wen, Applied Surface Science. 427, 281 (2018).
[47] R. Kumar, Nano-Micro Letters. 7.2, 97 (2015).
[48] H. Banimuslem, A. Hassan, T. Basova, A. Esenpınar, S. Tuncel, M. Durmuş, A. Gürek and V. Ahsen, Sensors and Actuators B: Chemical. 34, 207 (2015).